SECRET CONFIDENTIAL

OFFICE OF SCIENTIFIC RESEARCH & DEVELOPMENT

NATIONAL DEFENSE RESEARCH COMMITTEE.

DIVISION SIX-SECTION 6.1

WATER TUNNEL TESTS OF THE BRITISH "SQUID" PROJECTILE TYPE "C" WITH TWO ALTERNATE FLAT NOSES.

LIBRARY COPY
OF THE
HYDRODYNAMICS LABORATORY
CALIFORNIA INSTITUTE OF TECHNOLOGY
PASADENA 4, CALIFORNIA

Declassified on 7 Aug 1960 by authority of Sec. of Defense memo.

THE HIGH SPEED WATER TUNNEL
CALIFORNIA INSTITUTE OF TECHNOLOGY
PASADENA, CALIFORNIA.

SECTION No 6.1- sr- 207-938.

HML REP. No ND- 24.1

This document contains information affecting the National Defense of the United States within the meaning of the Espionage Act, 50 U.S.C., 31 and 32. Its transmission or the revelation of its contents in any manner to

COPY No 31 6-20-51

CONFIDENTIAL

~~CONFIDENTIAL~~
(~~SECRET~~)

OFFICE OF SCIENTIFIC RESEARCH AND DEVELOPMENT
NATIONAL DEFENSE RESEARCH COMMITTEE
DIVISION SIX — SECTION 6.1

WATER TUNNEL TESTS OF THE BRITISH "SQUID" PROJECTILE TYPE "C" WITH TWO ALTERNATE FLAT NOSES

BY

ROBERT T. KNAPP
OFFICIAL INVESTIGATOR

THE HIGH SPEED WATER TUNNEL
AT THE
CALIFORNIA INSTITUTE OF TECHNOLOGY
HYDRAULIC MACHINERY LABORATORY
PASADENA, CALIFORNIA

Section No. 6.1-sr-207-938
HML Report No. 24.1

Report Prepared By
H. L. Doolittle,
Hydraulic Engineer

November 29, 1943

SUMMARY

This report covers tests to determine the performance of the "Squid" with three designs of nose, designated No. 42, No. 45, and No. 46. Practically the only difference in the three noses is in the diameter of the flat face, these diameters being 7.90", 8.93", and 9.95", respectively. The following conclusions have been reached:

The projectile with Nose No. 45 gives the greatest restoring moment and CP eccentricity. The No. 42 Nose produced the least drag, although it is not much below that for the No. 45 Nose.

The values of the cavitation parameter, K, for incipient cavitation are 1.76, 2.08, and 2.40 for the No. 42, No. 45, and No. 46 Noses, respectively.

The calculated terminal velocities of the bomb with each of the three noses have the following approximate values in feet per second:

Nose No. 42 = 37

Nose No. 45 = 34

Nose No. 46 = 30

A reduction in drag of approximately 25% can be obtained by rounding the leading edges of the shroud ring and fins of the standard eight-fin tail.

Reducing the number of fins in the tail to four will give slightly better performance, including a 6% reduction in drag, and might result in advantages from the standpoint of manufacture.

On the basis of rough calculations it appears that if no air is present, vaporization and, therefore, a cavitation bubble cannot exist at greater values of submergence than the following:

with

Nose No. 42 - 26-1/2 feet

Nose No. 45 - 23 feet

Nose No. 46 - 19-1/2 feet

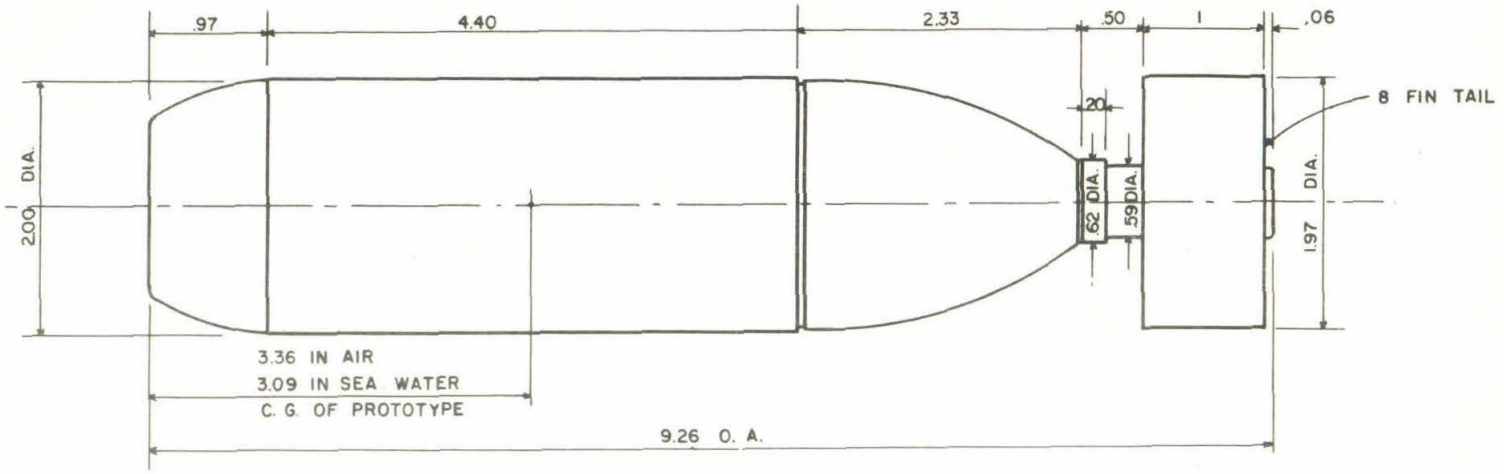

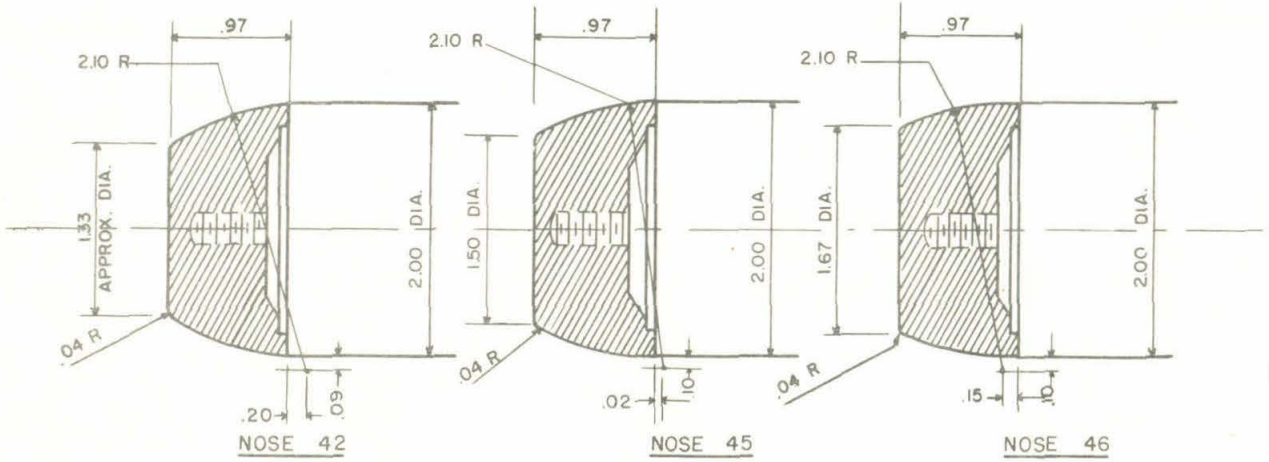

MODEL
AND
NOSE DETAILS

SCALE RATIO = 5.95

CIT – HML
DRG.- ND 24-1880 MS

FIGURE 1

SECRET

WATER TUNNEL TESTS OF THE BRITISH "SQUID" PROJECTILE TYPE "C" WITH TWO ALTERNATE FLAT NOSES

GENERAL DESCRIPTION

This report covers supplementary tests on the British "Squid" Type "C" Projectile, the original tests having been covered by Report Section No. 6.1-sr-207-933. These additional tests were for the purpose of determining the performance of the "Squid" with two different nose designs. The tests included determination of performance characteristics and photographs of cavitation effects for varying water pressures. For the sake of ready comparison, some of the data in the first report are repeated herein.

Appendix "A" gives a description of the various terms and symbols used, as well as a brief discussion of the requisite conditions for stability in a projectile. Appendix "B" gives a description of what has been termed the "Characteristic Chart". This is useful in determining the relative performance of various modifications in the design.

All curves of observed data have been faired and corrected for interference.

DESCRIPTION OF PROJECTILE

All data pertaining to the projectile covered by the first report apply to the projectiles covered by this report with the exception of the nose details. Figure 1 shows the dimensions of the model and the three nose designs that have been tested, these being designated Nos. 42, 45, and 46. It is seen that the principal difference is in the diameter of the flat face of the nose, being 7.90", 8.93", 9.95", respectively.

All models were tested with the same body and the standard eight-fin tail.

Data pertaining to the model and prototype are as follows:

Model Data:

Diameter	2"
Length overall	9.26"
Scale ratio	5.95"

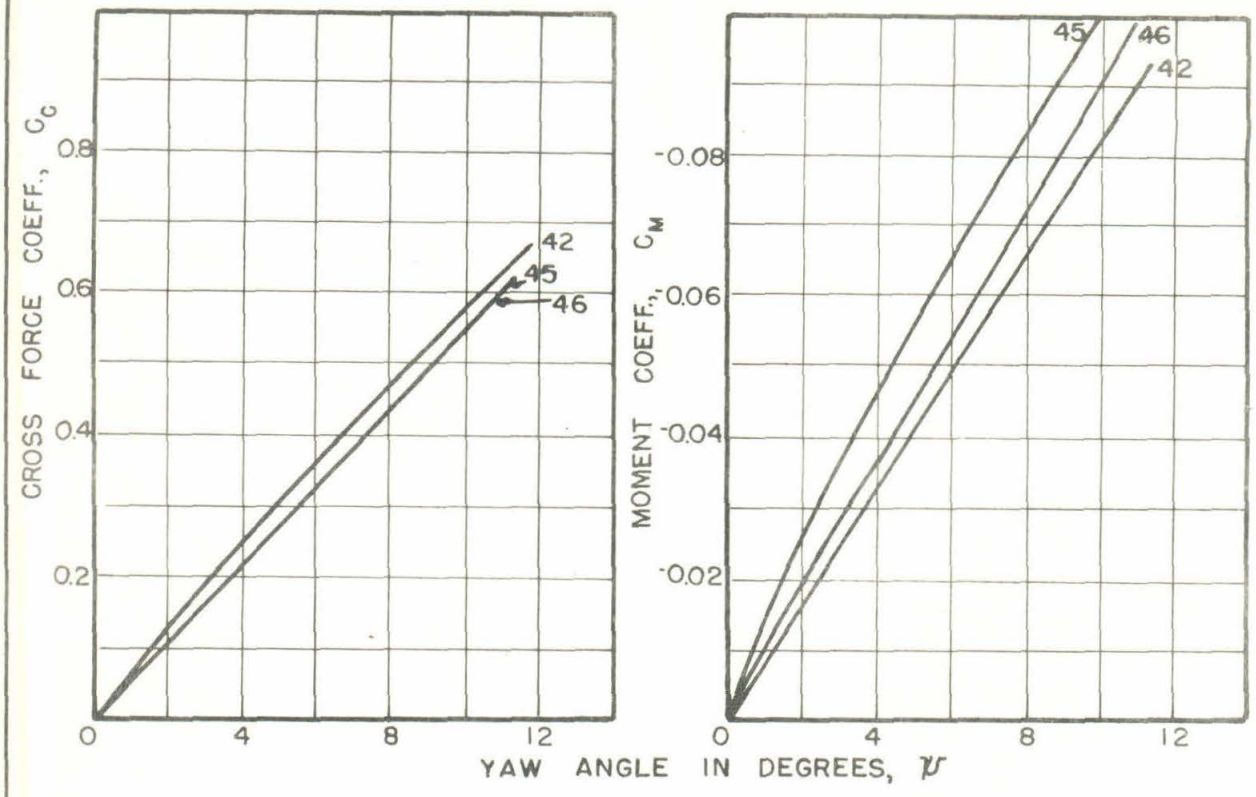

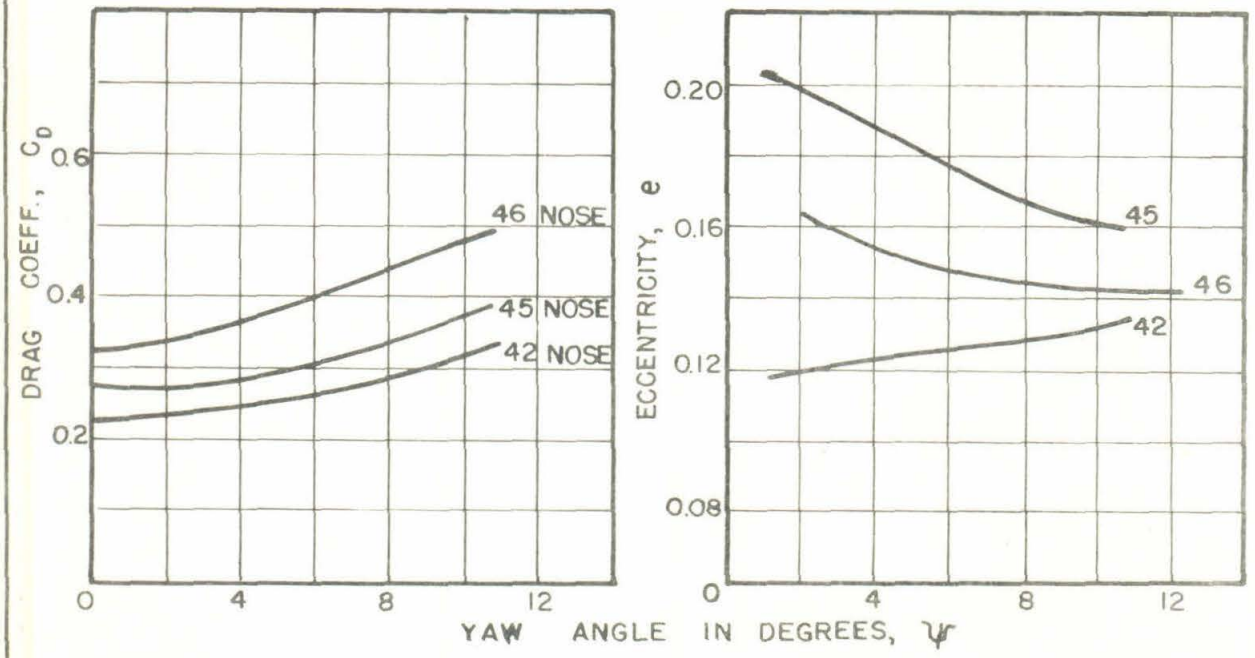

FORCE COEFFICIENTS

AND

C. P. ECCENTRICITY

CIT – HML
DRG.- ND 24-1881 LS

FIGURE 2

Prototype Data:

Diameter	11.9"
Length	54.8"
Total weight in air	386.4 lbs
Total weight in sea water	234 lbs
Distance from nose to	
Center of gravity in air	20"
Center of gravity in sea water	18.4"

PERFORMANCE CHARACTERISTICS

Tests were made in the High Speed Water Tunnel to determine the drag, cross force, and moment coefficients. The results are plotted on the curve sheet, Figure 2, which also includes the CP eccentricity. From these curves it is seen that there is little difference in the cross force coefficients for the three models. The drag increases materially with an increase in diameter of the flat face of the nose. At 10° yaw the drag for the No. 46 Nose is approximately 50% greater than for the No. 42 Nose.

It is interesting to note that the No. 45 Nose, having the intermediate diameter for the flat face, has the highest restoring moment as well as the greatest CP eccentricity. These differences are very substantial and it must be concluded that the No. 45 Nose design results in a much more stable projectile, although the drag is slightly greater than that obtained with the No. 42 Nose.

It is also of interest to observe that the CP eccentricity curves for the three designs seem to converge toward a common value with increasing yaw angles.

In making the tests to determine variation in drag with different values of K, described later in this report, one test was made with the eight-fin tail and an ellipsoidal nose. It was noted that this nose, which has a very low form drag, gave a reduction of about 15% in the drag coefficient over that obtained with the No. 42 Nose. In another test in this series the model was fitted with a four-fin tail very similar to the original eight-fin tail except that it was streamlined by rounding the leading edges of the fins and shroud ring. This slight change reduced the drag coefficient approximately 30%.

Another test was made with the No. 42 Nose and a tail exactly like the standard tail but with only four fins. It was found that this tail reduced the drag at least 6%, resulted in a moment slightly greater than that shown for the No. 45 Nose for yaws

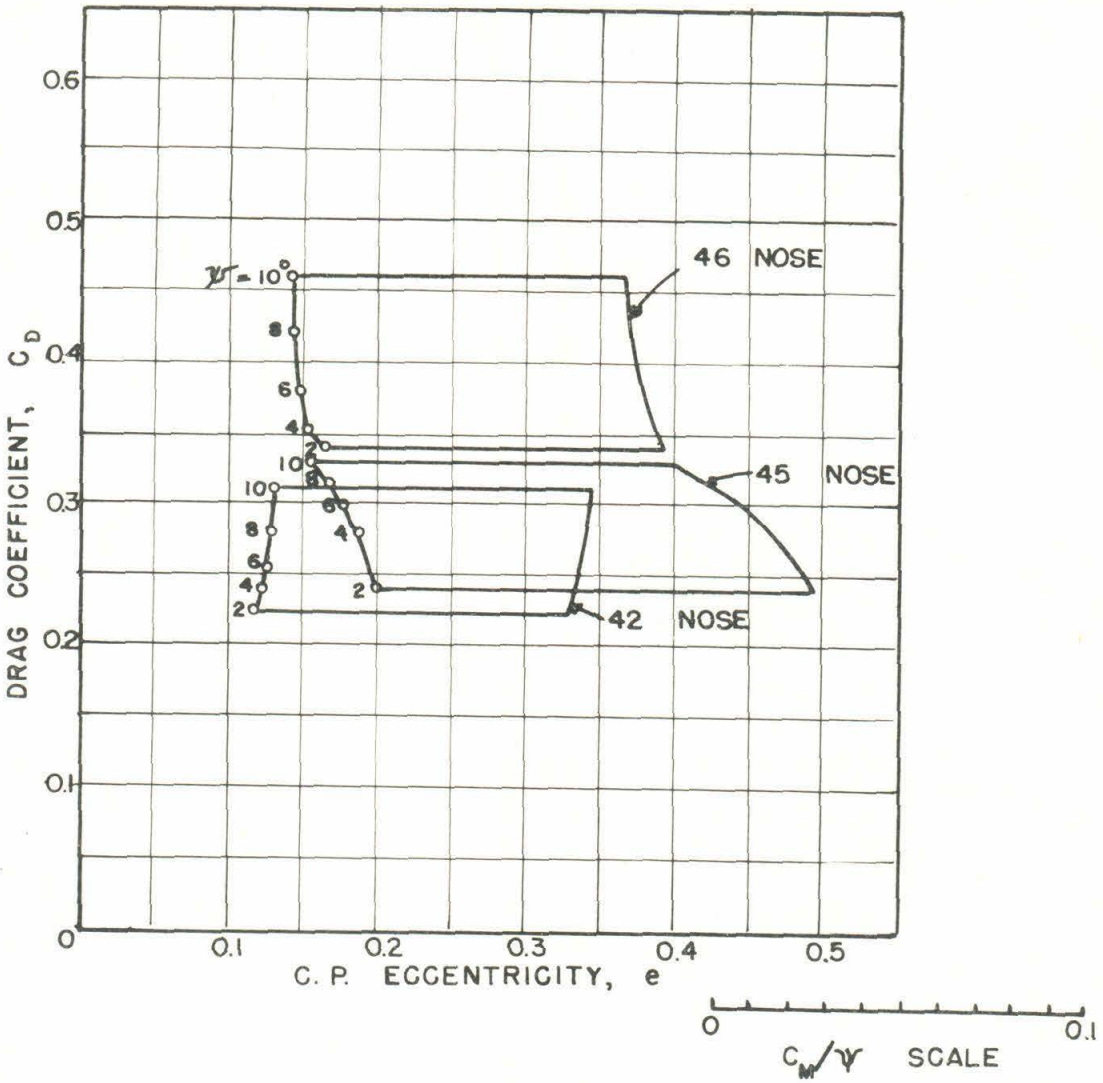

CHARACTERISTIC CHART

CIT — HML
DRG.— ND 24— 1882 LS

FIGURE 3

above 5°, and the CP eccentricity was nearly as large as for the No. 45 Nose. These tests showed that the four-fin tail would give somewhat better performance than the standard eight-fin tail and might result in some advantage from the standpoint of manufacture. As the leading edges of the fins and shroud ring of this four-fin tail were not rounded, it is reasonable to say that streamlining these edges would result in a total reduction of about 30% in the drag, as was found to be the case with the streamlined four-fin tail.

CHARACTERISTIC CHART

The Characteristic Chart, Figure 3, shows the relative values of drag coefficient, CP eccentricity, yaw angle, and rate of change of moment. This chart shows that Nose No. 45 produces little more drag than Nose No. 42, and considerably more restoring moment than the others, however, the change of moment with yaw is at a decreasing rate. All three designs of nose produce a fairly satisfactory degree of stability.

Appendix "B" gives a complete description of this chart.

TERMINAL VELOCITY

When the prototype projectile reaches its terminal velocity, its weight in water is equal to the drag force on the body. By using this relationship, a value for the drag coefficient at terminal velocity and also the formula for the drag coefficient, the terminal velocity can be calculated.

As no tests were made to determine the variation in drag with Reynolds number for the No. 45 and No. 46 Noses, these were derived from the tests of the No. 42 Nose. The tunnel tests with a 31 ft. water velocity and zero yaw showed that the drag coefficient with the No. 45 Nose was 0.045 higher than with the No. 42 Nose, and 0.095 higher with the No. 46 Nose. It was assumed that these same increases in drag would occur with the prototype at terminal velocity. As the tests with the No. 42 Nose showed the drag coefficient to be 0.224 at terminal velocity, on the above assumption the drag coefficients at terminal velocity would be 0.269 for the No. 45 Nose and 0.319 for the No. 46 Nose. By the method outlined above the calculated values for the terminal velocities in sea water are approximately 34 feet per second for the No. 45 Nose and 30 feet per second for the No. 46 Nose.

CAVITATION TESTS

A series of photographs was made of the model, with the No. 45 and No. 46 nose designs, to show cavitation effects. These photographs were taken with varying water pressures and a constant water velocity of 40 feet per second. Figures 6 to 18 show these photographs and, for purposes of comparison, similar photographs of the No. 42 Nose have been included as Figures 19 to 24. They have been arranged to show cavitation effects at approximately the same values of the cavitation parameter, K.

The cavitation parameter, K, is defined as follows:

$$K = \frac{P - P_v}{\rho \frac{V^2}{2}}$$

in which

P = Absolute static pressure in lbs per sq ft

P_v = Vapor pressure, at the corresponding water temperature, in lbs per sq ft

ρ = Mass density of the fluid in slugs per cu ft = $\frac{w}{g}$

w = Specific weight of the fluid in lbs per cu ft

g = Acceleration of gravity in ft per sec^2

V = Velocity of the projectile in ft per sec or velocity of the water, in model tests.

Comparing the three photographs in each vertical row, that is for the three models at approximately the same value of K, it is seen that the cavitation effect increases as the bluntness of the nose increases. In other words, the more blunt the nose, the higher the value of K for incipient cavitation.

Attention is called to Figures 11, 12, 17, and 18. These illustrate an unexpected phenomenon and one which has not been observed heretofore, as the Nos. 45 and 46 Noses are much more blunt than any others that have been tested and, consequently, the cavitation effect is much greater for a given pressure. Figure 12 represents practically the same condition as Figure 11 except the lighting has been changed to better show the outline of the cavitation bubble. The same is true of Figures 17 and 18. These photographs show clearly a definite change in the appearance and form of the cavitation bubble as low values of K are approached, the mass of small bubbles surrounding the model seems to disappear gradually and the cavitation envelope becomes translucent and of a more definite form. In Figure 10 this action is seen to be starting at the end of the nose. A careful examination of the photographs will disclose the outline of the model within the more or less transparent cavitation bubble.

FIG. 6
K = 1.05

FIG. 7
K = 0.65

NOSE NO. 46

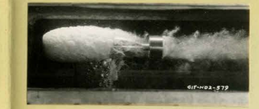

FIG. 8
K = 0.44

FIG. 9
K = 0.39

FIG. 10
K = 0.37

FIG. 11
K = 0.37

FIG. 12
K = 0.36

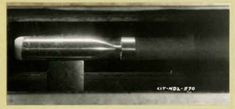

FIG. 13
K = 1.00

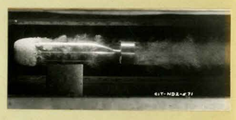

FIG. 14
K = 0.69

NOSE NO. 45

FIG. 15
K = 0.52

FIG. 16
K = 0.40

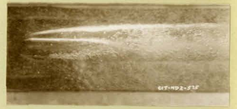

FIG. 17
K = 0.35

FIG. 18
K = 0.34

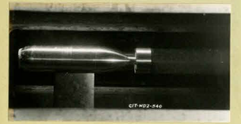

FIG. 19
K = 1.03

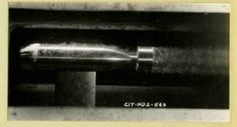

FIG. 20
K = 0.68

NOSE NO. 42

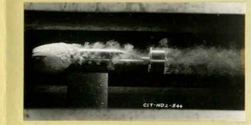

FIG. 21
K = 0.52

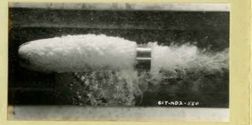

FIG. 22
K = 0.39

FIG. 23
K = 0.37 (+)

FIG. 24
K = 0.37 (-)

PHOTOGRAPHS OF
CAVITATION TESTS

FIGURES 6 TO 24

CIT – HML
DRG – ND 24 – 1883 MS

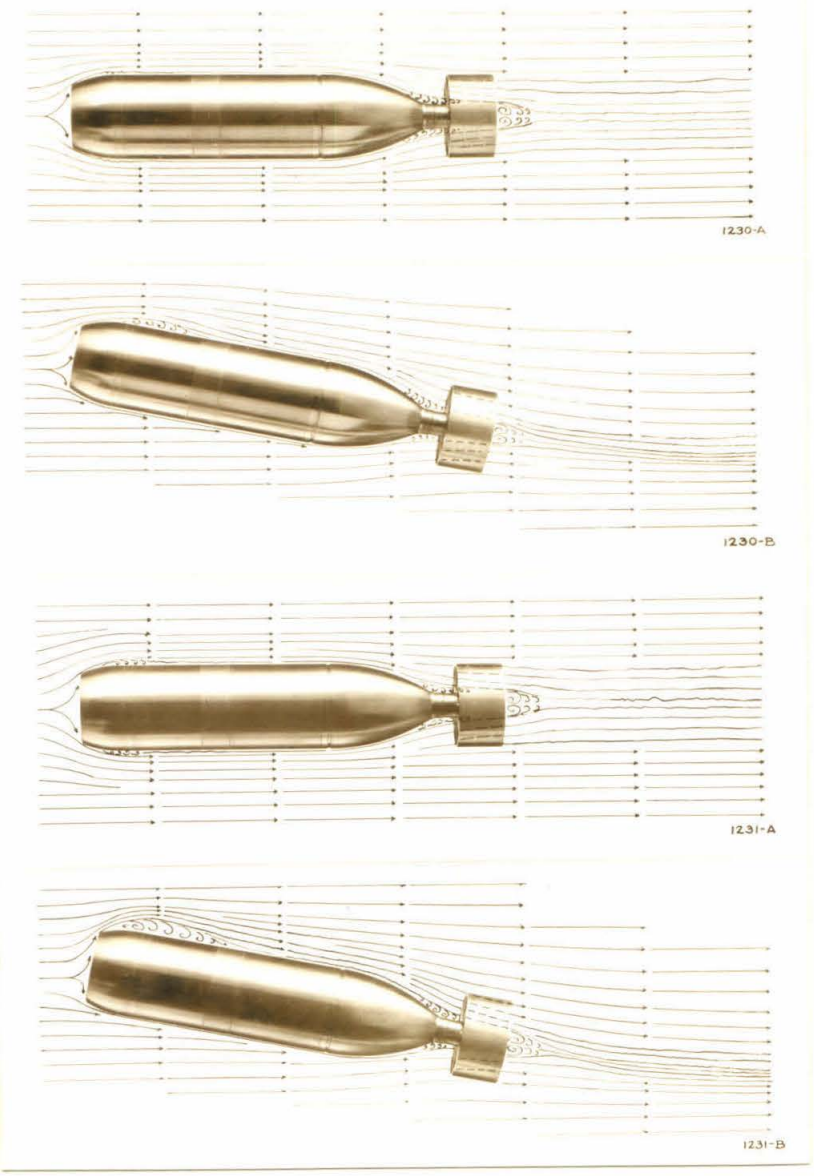

FIGURE 25
NO. 45 NOSE
YAW ANGLE 0° AND 12°

FIGURE 26
NO. 46 NOSE
YAW ANGLE 0° AND 12°

FLOW DRAWINGS

The flow drawings, Figures 25 and 26, show the disturbance created by Noses No. 45 and 46. As would be expected, the more blunt nose, No. 46, creates the greater disturbance at all values of yaw angle. This is also borne out by the drag determinations, since the noses that create the largest disturbance also have the largest drag. Comparing these flow drawings with those of Nose No. 42, it is seen that the No. 42 design is superior to either of the others from the standpoint of smoothness of flow pattern.

An examination of the flow about the tail shows that the afterbody causes some disturbance which, in turn, results in an increase in drag although it is believed this increase is of small magnitude

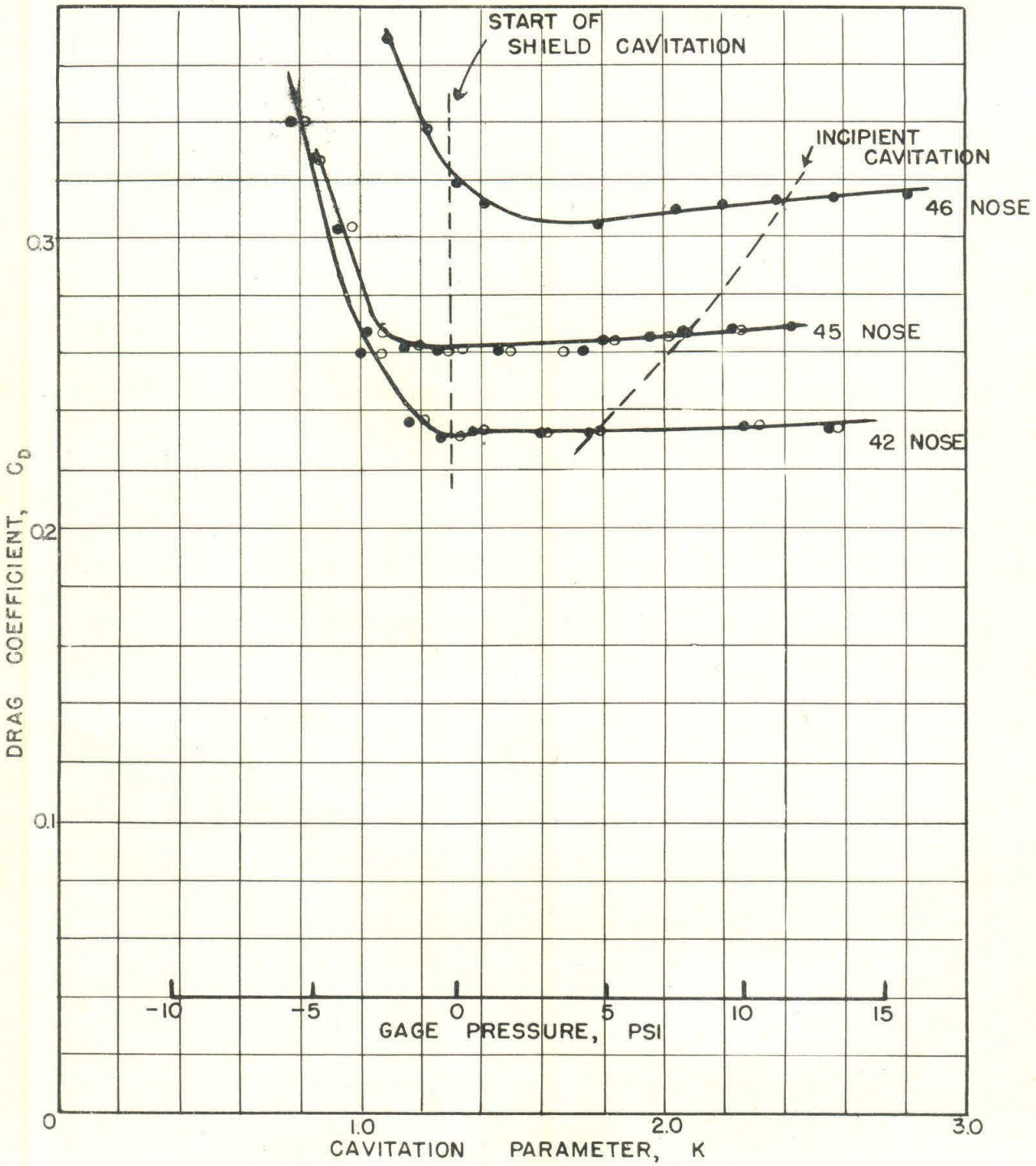

DRAG COEFFICIENT
AND
CAVITATION PARAMETER

CIT - HML
DRG.-ND 24 - 1884 LS

FIGURE 27

CAVITATION AND DRAG

A series of tests was made to determine the variation in drag with K for the different noses. The results of these tests are shown in Figure 27. The dotted line indicates that incipient cavitation occurs at higher values of K as the bluntness of the nose increases.

These curves show the same rapid rise in drag for values of K below about 1.3. There was some suspicion that this effect might be largely due to interference caused by cavitation on the support shield. In order to check this, a run was made with the model fitted with an ellipsoidal nose and a streamlined tail, both of which cavitated at very low values of K. This test showed the same rapid rise in drag below K = 1.2 so the conclusion was reached that this could not be due entirely to the cavitation of the model.

That the sudden rise in drag cannot be charged entirely to the effect of the support shield is shown by the test of the model with the No. 46 Nose. Here the drag begins to rise at a value of K = 1.7, whereas the shield does not start cavitating before a value of K = 1.3 is reached. No method is available at present for evaluating the effect of shield cavitation on this increase in drag. It is certain this increase occurs but the exact form of the curve for low values of K is not known.

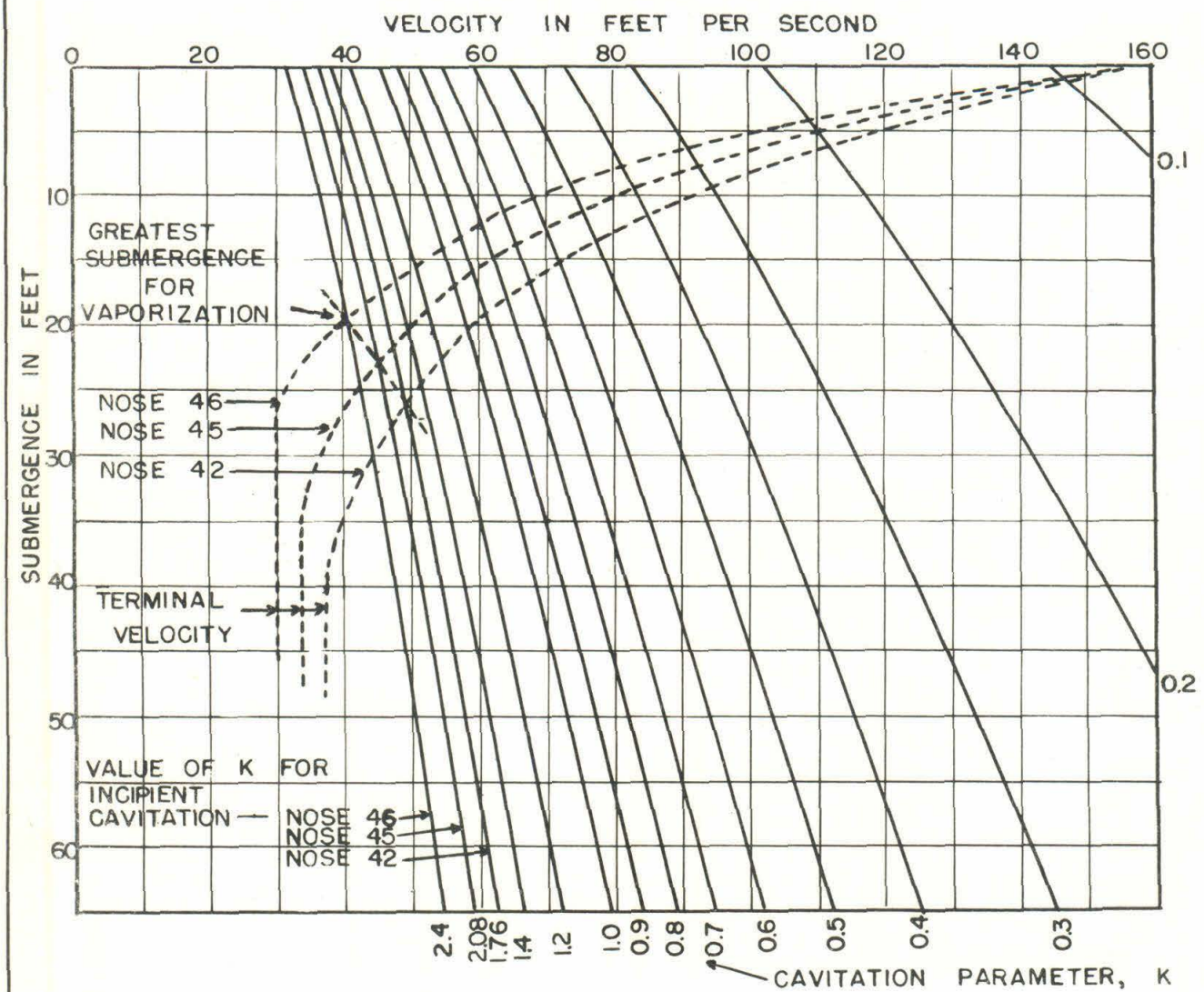

RELATION BETWEEN

VELOCITY, SUBMERGENCE AND K

CIT — HML

DRG.- ND 24 - 1885 LS

FIGURE 28

CAVITATION AND SUBMERGENCE

It is understood that this projectile enters the water at a velocity of approximately 160 feet per second and at an angle of 45°. Bodies with hemispherical noses appear to have an effective drag coefficient of about 0.67 at entrance. In this discussion it has been assumed that this value of 0.67 for the drag coefficient applies to the "Squid" with the No. 42 Nose, which has a 7.90" diameter flat face. The drag coefficients for the other noses have been assumed to be proportional to the areas of the flat faces. This gives drag coefficients of 0.85 for the No. 45 Nose and 1.05 for the No. 46 Nose. These coefficients are probably much lower than the actual values. It was further assumed that the drag coefficient decreases linearly with increasing values of the cavitation parameter, K, until it reaches a terminal value for the prototype at K = 1.25, approximately.

On the basis of these assumptions the velocity-submergence relation has been calculated for the projectile with the three nose designs. The results of these calculations are shown in Figure 28. In calculating the performance of the projectile, after entrance, it was assumed that the pressure in the bubble was equal to the vapor pressure corresponding to a temperature of 50° Fahrenheit. While these curves are purely speculative, it is believed they are of some value in giving an approximate idea of the projectile performance.

The curves in Figure 28 show that the submergence at which terminal velocity is reached is decreased with increasing bluntness of nose.

The intersection of the projectile performance curves with their respective curves of K for incipient cavitation indicates the submergence below which no vaporization can take place. It is not possible to say, with the present knowledge of the subject, whether or not an air bubble can exist below this submergence; however, it is proper to say that this submergence represents the lower limit for the existance of a cavitation bubble if no air is present. It is believed that all of the assumptions made for the purpose of calculating the velocity-submergence-K relationship are conservative and, consequently, the depths beyond which vaporization will not occur will be less than shown. For the same reason the depths at which terminal velocity is reached also will be less than shown.

CONFIDENTIAL

THE HIGH SPEED WATER TUNNEL
AT THE
CALIFORNIA INSTITUTE OF TECHNOLOGY

APPENDIX A

DEFINITIONS

YAW ANGLE

The angle which the axis of the model makes with the direction of flow. Looking down on the model, yaw angles in a counter-clockwise direction are negative (-) and in a clockwise direction, positive (+).

MOMENTS

Moments tending to rotate the model in a counter-clockwise direction (when looking down on the model) are negative (-), and those causing clockwise rotation, positive (+).

In accordance with this sign convention a moment has a destabilizing effect when it has the same sign as the yaw angle.

In all model tests the moment is measured about the point of support.

Moments about the center of gravity have the symbol, M_{cg}.

DRAG

The force, in pounds, exerted on the model parallel with the direction of flow.

CROSS FORCE

The force, in pounds, exerted on the model normal to the direction of flow. A positive cross force is defined as one acting in the same direction as the displacement of the projectile nose for a positive yaw.

NORMAL COMPONENT

The sum of the components of the drag and cross force acting normal to the axis of the model. The value of the normal component is given by the following:

$$N = (D \sin \psi + C \cos \psi)$$

in which

N = Normal component in lbs

D = Drag in lbs

C = Cross force in lbs

ψ = Yaw angle in degrees

CONFIDENTIAL

CENTER OF PRESSURE

The point in the axis of the model at which the resultant of all forces acting on the model is applied. This has the symbol (CP).

CENTER-OF-PRESSURE ECCENTRICITY

The distance between the center of pressure (CP) and the center of gravity (CG) expressed as a decimal fraction of the length (L) of the model. The center-of-pressure eccentricity (e) is derived as follows:

$$e = \frac{(L_{cp} - L_{cg})}{L} = \frac{1}{L} \quad \frac{M_{cg}}{N}$$

in which

e = Center-of-pressure eccentricity

L = Length of model in feet

L_{cg} = Distance from nose of projectile to CG in feet

L_{cp} = Distance from nose of projectile to CP in feet

COEFFICIENTS

The three force coefficients used are derived as follows:

Drag coefficient, $$C_D = \frac{D}{\rho \frac{V^2}{2} A_D}$$

Cross force coefficient, $$C_C = \frac{C}{\rho \frac{V^2}{2} A_D}$$

Moment Coefficient, $$C_M = \frac{M}{\rho \frac{V^2}{2} A_D L}$$

in which

D = Measured drag force in lbs

C = Measured cross force in lbs

ρ = Density of the fluid in slugs/cu ft

w = Specific weight of the fluid in lbs/cu ft

g = Acceleration of gravity in ft/sec^2

A_D = Area in sq ft of a cross section at the cylindrical portion of the projectile taken normal to the geometric axis of the projectile

V = Mean relative velocity between the water and the projectile in ft/sec

M = moment in foot-lbs measured about any particular point on the geometric axis of the projectile

L = overall length of the projectile in feet

GENERAL DISCUSSION

The curves of force and moment coefficients and of center-of-pressure distance plotted as functions of the yaw angle are useful for a discussion of the stability of projectiles. Since these tunnel tests are made under steady flow conditions, the results will only indicate the tendency of the projectile to return to or move away from the equilibrium position after a disturbance. Adopting aerodynamic usage, a projectile is said to be "statically" stable if it tends to return to equilibrium when disturbed. In the discussion of static stability the actual motion following the perturbation is not considered at all. In fact, a projectile may oscillate about the equilibrium position without ever remaining in it. In this case the projectile would be statically stable even though "dynamically" unstable. For a complete discussion of the mode of motion to be expected following a perturbation, the "dynamic" stability, additional information is necessary.

The condition for equilibrium is satisfied if C_M, calculated about the CG is equal to zero. In general, for projectiles with axial symmetry the moment is zero at $\psi = 0^o$, so that for equilibrium the projectile is oriented with its axis parallel to the direction of motion. If the projectile is rotated from the equilibrium position so as to give it a positive yaw angle, it is necessary that it have a negative moment coefficient, according to the sign convention adopted, in order that it be statically stable. Thus, a negative slope of the curve, C_M, vs. ψ corresponds to static stability, and a positive slope corresponds to instability. The degree of stability or instability is indicated by the magnitude of the slope. The same conclusions are obtained by interpreting the center-of-pressure curves. For symmetrical projectiles, if the center of pressure falls behind the center of gravity, a restoring moment exists and the projectile is statically stable. If the CP lies ahead of the CG, the moment is non-restoring and the projectile is statically unstable. The degree of stability or instability is indicated by the distance between the center of gravity and center of pressure.

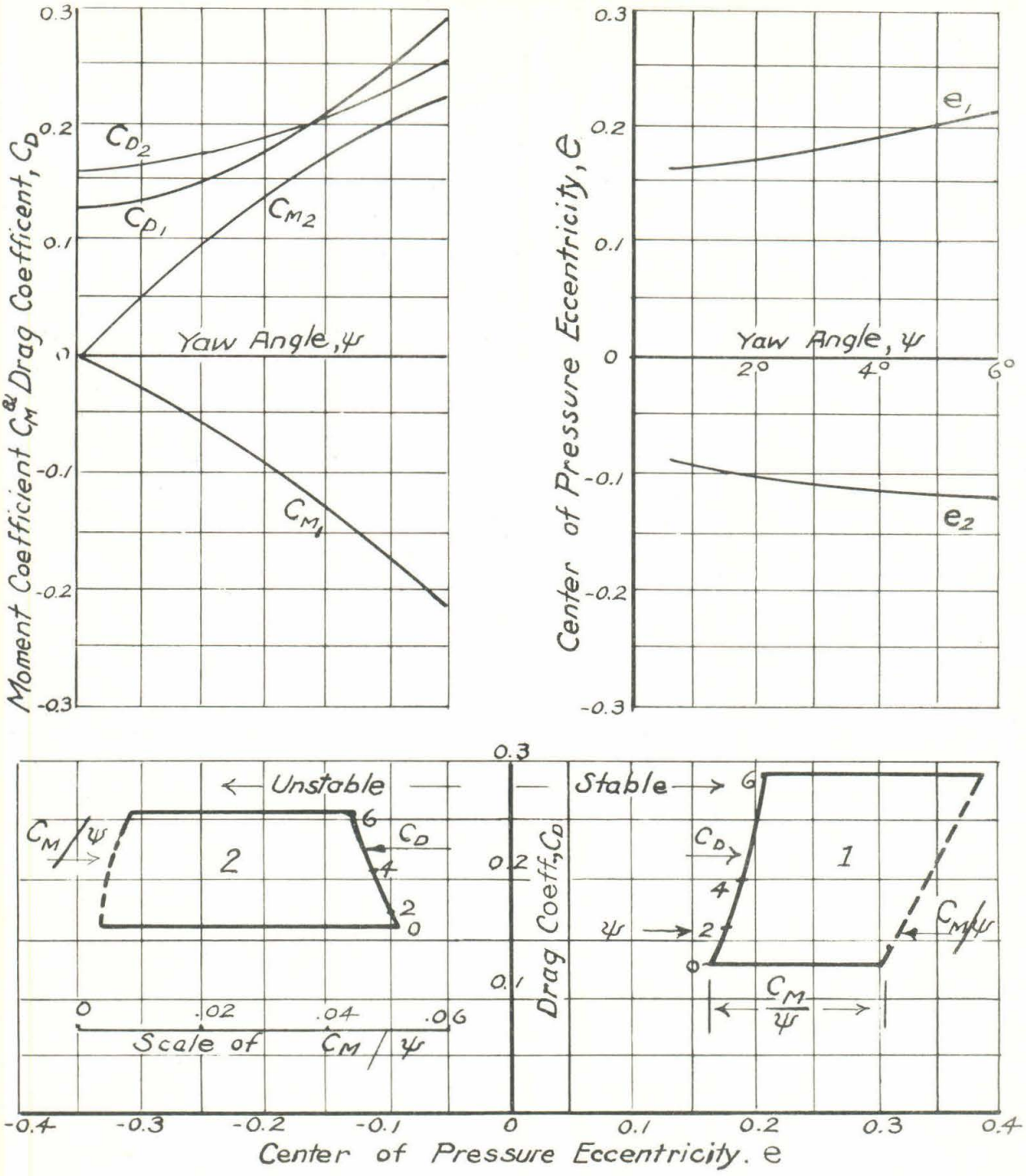

TYPICAL CHARACTERISTIC CHART

The California Institute of Technology---High Speed Water Tunnel.

DRG:-1024-1671-L

THE HIGH SPEED WATER TUNNEL
AT THE
CALIFORNIA INSTITUTE OF TECHNOLOGY

APPENDIX B

DESCRIPTION OF CHARACTERISTIC CHART

The attached curve sheet shows typical curves for drag and moment coefficients and, also, center-of-pressure eccentricity, all varying with the yaw angle. Two cases have been assumed, indicated by the subscripts (1) and (2). These curves are selected merely to illustrate method of plotting the chart and do not represent data on the projectile discussed in this report.

In order to obtain a better visualization of the performance indicated by the curves mentioned above, the "Characteristic Chart", shown at the bottom of the sheet, has been devised. In this chart the drag coefficient, C_D, is first plotted against the CP eccentricity, e. On this C_D curve are points opposite which are figures indicating the yaw angle, ψ. This C_D curve shows the variation in drag and CP eccentricity with yaw angle. Also, the position of the curve at the right or left of the vertical axis (+ e or – e) indicates whether or not the projectile is stable or unstable, in other words, whether the CP lies aft or forward of the center of gravity.

On this same chart is plotted the quantity C_M/ψ which gives an indication of the change in the moment coefficient, C_M, with varying yaw angle. This is done by dividing the C_M by the yaw in degrees and plotting these values, C_M/ψ, to a suitable scale, horizontally from the points representing the yaw angle. (For each yaw angle the zero for the C_M/ψ scale is at the C_D curve).

The "Characteristic Chart" is useful as it gives a fairly complete picture of the variation of three important characteristics of the projectile with changes in yaw angle. It is seen that Case 1 has much less increase in drag than Case 2. Also, that the CP eccentricity in Case 1 increases with the yaw and is positive, and therefore, tends to increase stability. In addition to this, the C_M is increasing at an *increasing* rate, indicating a proportional increase in restoring moment with increasing yaw angles. This is an additional stabilizing factor.

In Case 2 the opposite characteristics of Case 1 are indicated. Here, there is a greater increase in drag with increase in yaw; also, the CP eccentricity, which is negative, increases with the yaw, thus tending to decrease stability. The change in moment coefficient occurs at a *decreasing* rate, indicating a proportional decrease in restoring moment with increasing yaw. This is a destabilizing factor.